

INVESTIGATION ON WAKE GALLOPING OF CABLE WITH SPIRAL PROTUBERANCES BY PRESSURE MEASUREMENTS

京都大学	学生員	○ Tung Quang Do	京都大学	正会員	八木 知己
京都大学	正会員	野口 恭平	京都大学		福島 温樹
京都大学		Thu Minh Dao	京都大学	学生員	桑原 彰吾

1. INTRODUCTION

Wake-induced vibration is a major concern for cables arranged in parallel. There are several possible wake-induced vibration responses depending on the arrangement of the cables. This study focuses on wake galloping (or vertical flutter) of 2 relatively close cables. A previous study has shown that a cable with 12 spiral protuberances at winding angle of 27° (hereinafter called spiral cable) could partially suppress wake induced vibration in parallel cables¹⁾. However, the suppression mechanism is yet to be investigated. This study discusses wake galloping characteristics of spiral cable at high reduced wind velocity based on surface pressure obtained from wind tunnel tests.

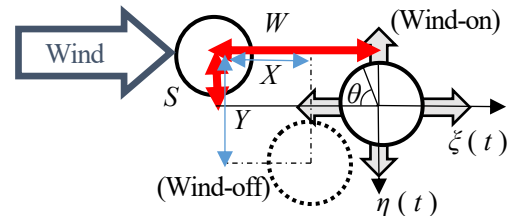


Fig. 1 Parallel cables arrangement in crossflow

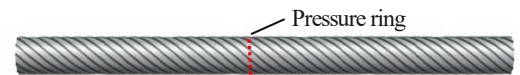


Fig. 2 Spiral cable model

2. WAKE GALLOPING RESPONSES OF PARRALEL CABLES AT HIGH WIND VELOCITY

Fig. 1 shows the arrangement and coordinate systems for 2 parallel cables. (X, Y) and (S, W) denote the distance of the downstream cable from the upstream cable in wind-off (initial condition) and wind-on condition respectively; θ represents the angular position of the pressure taps; η and ξ are the displacements in vertical and horizontal direction. The main focus of this study is placed on $(X/D, Y/D) = (3.0, 0.5)$ which is equivalent to $(S/D, W/D) = (3.0, 0.3)$ and at reduced wind velocity of $U/fD > 100$ (corresponding to $Re > 2 \times 10^4$ – the supercritical region for a single spiral cable¹⁾) in view of practical engineering applications as well as minimizing the effect of Reynolds dependency. In this particular arrangement where both cables were smooth circular cylinder, denoted by Circular (upstream) – Circular (downstream) in Fig. 3, large amplitude vertical flutter was observed in the downstream cable at $U/fD > 100$ (the shaded areas in Fig. 3). A downstream spiral cable was able to suppress the vibration at high reduced wind velocity. It seemed that the configuration of the downstream cable strongly dictated its stability regardless of the configuration of the upstream one as there was no significant difference between the responses of Circular – Spiral and Spiral – Spiral.

Flutter analysis revealed that the vibration observed in Circular – Circular was driven by unsteady aerodynamic derivative H_1^* which is defined in Eq. (1)²⁾.

$$H_1^* = -\frac{L_{\eta 0} \sin \psi_{L\eta}}{\rho(0.5D)^2 \omega^2 \eta_0} \quad (1)$$

where: ρ is the air density [kg/m^3]; D is the diameter of the cable [m]; ω is the angular frequency of the forced vibration [rad/s]; $L_{\eta 0}$ is the amplitude of unsteady lift force per unit length [N/m]; $\psi_{L\eta}$ is the phase lag between vertical displacement and the unsteady lift force; η_0 is the amplitude of the vertical motion in forced vibration. $H_1^* > 0$ describes negative aerodynamic damping in the vertical direction and thus, indicates galloping. Additionally, $H_1^* > 0$ was shown to have a major role in the 2DOF flutter with dominant vertical vibration of Circular – Circular seen in Fig. 3²⁾.

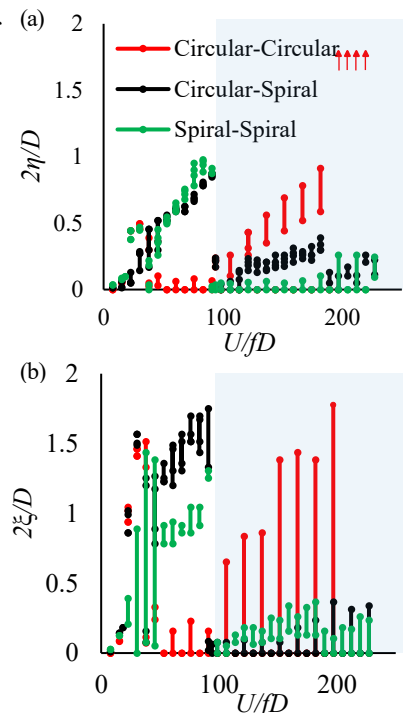


Fig. 3 Free vibration responses of downstream cable in (a) vertical and (b) horizontal direction

Keywords: wake galloping, parallel cables, cable with spiral protuberances.

連絡先: 〒615-8540 京都市 西京区 京都大学桂 京都大学工学研究科社会基盤工学専攻 Tel: 075-383-317

3. WAKE GALLOPING CHARACTERISTICS OF PARALLEL CABLES

In this section, wake galloping suppression mechanism of spiral cable is discussed based on static and unsteady pressure in $(S/D, W/D)=(3.0, 0.3)$ at $U/fD=183$ ($Re=4.2 \times 10^4$).

Fig. 4 shows the distribution of surface pressure coefficient C_p on the circumference of the downstream cable. The high negative pressure at $0^\circ \leq \theta \leq 120^\circ$ in Circular – Circular originated from gap flow³⁾, which is a high-speed flow in the gap between two parallel cables in certain arrangements. Gap flow generated non-zero lift force on the downstream cable and directed it toward the upstream one. In the case of downstream spiral cable, this negative pressure region was significantly reduced. Thus, the spiral protuberances on the downstream cable must have somehow suppressed the gap flow.

Fig. 5 shows H_1^* calculated at each pressure tap on the circumference of the downstream cable. In the case of downstream smooth cable, $H_1^* > 0$ was found at the outer region of the cable ($180^\circ \leq \theta \leq 360^\circ$). H_1^* was maximum at $255^\circ \leq \theta \leq 270^\circ$. The majority of $H_1^* > 0$ did not come from the gap flow region but the outer region. As shown in Eq. (1), H_1^* was decided by $L_{\eta 0}$ (integrated from C_p) and $\psi_{L\eta}$. At the outer region, although negative pressure was not as significant as in the gap flow region, there existed a remarkable phase lag. Time series $C_p(t)$ of the downstream smooth cable is presented in Fig. 6a. High negative pressure (denoted by the dark blue region) at the inner region did not persistently exist throughout the whole period T but rather switched intermittently between the inner region ($0^\circ \leq \theta \leq 90^\circ$) and the outer region ($255^\circ \leq \theta \leq 270^\circ$). It seemed that the gap flow periodically reduced its strength as it switched to the outer flow. This flow switching phenomenon probably caused the significant phase lag at the outer region.

Such switching phenomenon, however, was not observed in the case of downstream spiral cable (Fig. 6b and 6c). The spiral protuberances must have suppressed the gap flow so that no switching occurred. Consequently, not only did negative pressure get minimized but the phase lag was also reduced and H_1^* decreased. Fig. 5 reaffirmed the action of the downstream spiral cable was consistent regardless of the configuration of the upstream cable as H_1^* profiles in Circular – Spiral and Spiral – Spiral are very close in shape. It should be noted that there existed variation in the unsteady pressure field along the span of the spiral cable. However, wake galloping and its suppression mechanism could be explained in the view of 2-dimensional pressure characteristics because the sign of H_1^* remained consistent spanwise.

4. CONCLUSIONS

1) Gap flow did not directly drive wake galloping but the flow switching phenomenon between gap flow and outer flow.

2) By suppressing gap flow and eventually preventing flow switching, a downstream cable with spiral protuberances was able to stabilize itself against wake galloping at high reduced wind velocity in the arrangement $(S/D, W/D)=(3.0, 0.3)$.

ACKNOWLEDGEMENT

This work was partially supported by JSPS KAKENHI Grant number 20H02232.

REFERENCES 1) Do et al.: 令和2年度土木学会全国大会第75回年次学術講演会, I-45, 2020. 2) 袁ら: 平成29年度日本風工学会年次研究発表会梗概集, 2017. 3) Zdravkovich.: J. Wind Eng. Ind. Aerodyn., 28(1-3), 183-199, 1988.

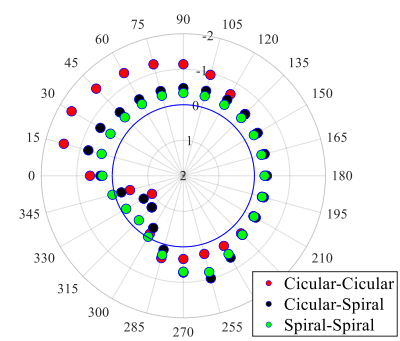


Fig. 4 C_p in circumferential direction at $U/fD=183$

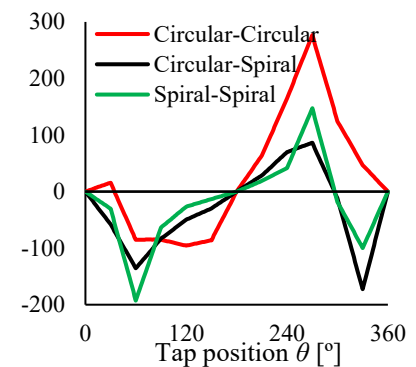


Fig. 5 H_1^* in circumferential direction at $U/fD=183$

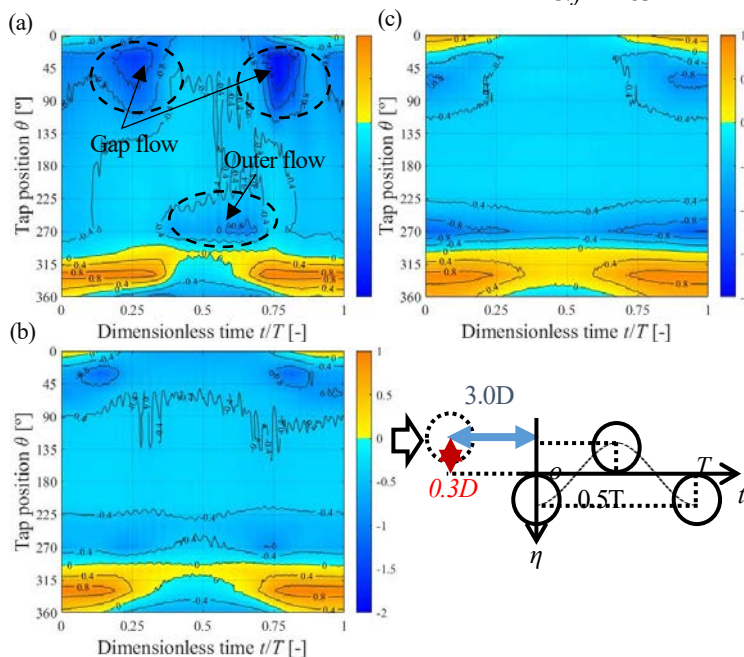


Fig. 6 Time series $C_p(t)$ of downstream cable in one period T of the forced vibration

(a) Circular – Circular, (b) Circular – Spiral and (c) Spiral – Spiral